Mechanism of singlet oxygen generation during catalytic decomposition of methyl(trifluoromethyl)dioxirane by chloride ions

M. Yu. Ovchinnikov, S. L. Khursan, and D. V. Kazakov*

Institute of Organic Chemistry, Ufa Research Center of the Russian Academy of Sciences, 71 prosp. Oktyabrya, 450054 Ufa, Russian Federation. Fax: +7 (347) 235 6066. E-mail: chemlum@anrb.ru

The mechanism of the chloride ion-induced catalytic decomposition of methyl(trifluoromethyl)dioxirane in trifluoroacetone was studied at the MP4//MP2/6-31+G(d) level of theory. The solvated chloride ion interacts with dioxirane to form an ion-dipole pair, which is transformed into the key intermediate $ClO—C(Me)(CF_3)—O^-$ acting as a chain carrier in the catalytic decomposition of dioxirane. The generation of singlet oxygen occurs during the transformations of this intermediate on the singlet potential energy surface.

Key words: catalysis, nucleophilic substitution, reaction mechanism, singlet oxygen, dioxiranes, quantum chemical calculations, MP4//MP2/6-31+G(d), G3MP2B3, NBO, and AIM methods.

The generation of singlet oxygen ($^1O_2$) in reactions of three-membered cyclic peroxides, *viz.*, dioxiranes,[1—3] was reported for the first time in the study,[4] in which the chemiluminescence characteristic of $^1O_2$ was observed in the IR spectral region[5] in the course of oxidation of 4-(dimethylamino)pyridine with dimethyldioxirane (DMD). The resulting N-oxide caused the rapid decomposition of peroxide. Some other N-oxides also cause the decomposition of DMD and methyl(trifluoromethyl)dioxirane (TFD, **1**) accompanied by IR chemiluminescence of singlet oxygen.

The scheme of the generation of $^1O_2$ was proposed in the studies.[4,6] According to this scheme, the nucleophilic attack of the negatively charged oxygen atom of N-oxide on the peroxide bond of dioxirane giving the peroxide intermediate, *viz.*, the adduct of dioxirane and $R_3N^+—O^-$, is responsible for the decomposition of dioxiranes and the generation of singlet oxygen. More recently, based on the available experimental data, the similar mechanism of the catalysis was proposed for the anion-induced decomposition of dioxiranes,[7—9] which are new efficient systems for the generation of $^1O_2$ (Scheme 1).

Unlike the reactions of dioxiranes with tertiary amines, the anion-induced catalytic decomposition of peroxides is characterized by high yields of $^1O_2$. In the case of chloride ions, the yield of $^1O_2$ is 97 and 69% for DMD and TFD, respectively.[9]

Taking into account the high yields of singlet oxygen and the important role of dioxiranes in organic synthesis[1—3] and chemiluminescence of oxidation reactions,[2,10—12] detailed data on the mechanism of the reactions of dioxiranes with anions are of considerable interest. These data can provide deeper insight into the generation of ex-

Scheme 1

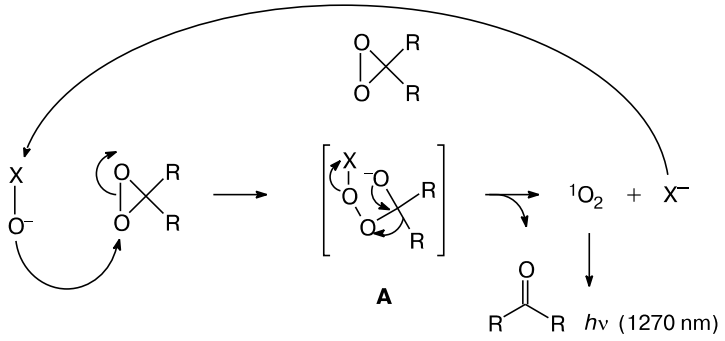

X = Cl, Br, I, Me_3CO, OH

Published in Russian in *Izvestiya Akademii Nauk. Seriya Khimicheskaya,* No. 1, pp. 29—36, January, 2011.

cited states in reactions of peroxides, can help in understanding the factors having an effect on the stability of dioxiranes in solutions, and can be useful in the examination of the possibility of the practical application of these reactions, for example, as a source of $^1O_2$ in chemical lasers or in organic synthesis.

In our previous study, we have investigated the mechanism of the chloride ion-induced decomposition of DMD by *ab initio* methods and proposed the scheme explaining the generation of singlet oxygen.[13] In the present study, we investigated the mechanism of the reaction of TFD, which is the most reactive dioxirane, with Cl^- ions by quantum chemical methods and performed the comparative analysis of the results to reveal the influence of the nature of dioxirane on the catalytic decomposition and the efficiency of the generation of $^1O_2$.

Calculation procedures

The full optimization of all structures, the solution of the vibration problem, and the thorough investigation of the potential energy surface of the reaction, including the relaxed scan and the intrinsic reaction coordinate (IRC) scan, have been performed as described in the previous study[13] by the second- and fourth-order Möller—Plesset perturbation theory (MP2 and MP4, respectively), the quadratic configuration interaction with single and double excitation (QCISD), and the coupled cluster (CC) methods. The wave-functions of all compounds, except for the oxygen molecule, were constructed by the restricted Hartree—Fock method. The basis set superposition error was estimated by the counterpoise method. The energy parameters for the chloride ion-induced decomposition of TFD were reduced to 298 K in the calculations of the zero-point vibrational energy and thermal corrections for all the compounds under study. The transition states are marked with the sign "≠"; the other stationary points, which are not marked with this sign, correspond to equilibrium structures.

The choice of the methods of investigations was explained in detail in the earlier study of the related reaction of DMD with chloride ions.[13] The examination of different quantum chemical levels of theory for the reliability and reproducibility of the geometric and energy characteristics of the reaction under study confirmed the previous conclusions that the extension of the basis set (starting with 6-31+G(d)) has virtually no effect on the results of calculations and that it is reasonable to use the QCISD and MP2 methods for the optimization of the structures and the electron correlation correction. Hence, we chose the MP2 perturbation theory method, which is less time-consuming than the QCISD method, as the main method of investigations. The energies of the structures were improved by the MP4 method (SDTQ).

The adiabatic electron affinity was calculated by the G3MP2B3 method[14] as the difference between the standard enthalpies of formation of the neutral species and its coupled anion. The electron density analysis was performed by the natural bond orbital (NBO)[15] and Bader's Atoms in Molecules (AIM)[16] methods. All calculations were carried out with the use of the Gaussian 03 Revision-D02 program package.[17]

Results and Discussion

Geometric parameters. The thorough scan of the potential energy surface for the reaction of compound **1** with chloride ions in trifluoroacetone (TFA) revealed compounds **2**, **3** (Fig. 1), **7**, and **8**,* transition states $\mathbf{4}^{\neq}$ and $\mathbf{9}^{\neq}$, and intermediates **5** (its protonated form **6**), **10**, and **11**. The main geometric parameters of all these structures are presented in Tables 1 and 2. Structures $\mathbf{4}^{\neq}$ and $\mathbf{9}^{\neq}$ are characterized by imaginary vibrational frequencies of −63 and −135 cm^{-1}, respectively, reflecting the displacements of the nuclei along the reaction coordinate. The presence of the single imaginary frequency and the energy profile determined by IRC calculations confirmed that the transition states do occur.

Energies of ion-dipole interactions and the enthalpies of formation of compounds 2, 3, 7, and 8. Structures **2**, **3**, **7**, and **8** deserve more detailed analysis. These structures consist of an ion (chloride anion or intermediate **5**) and a molecule (TFA or dioxirane **1**), the anion being oriented in the direction opposite to the oxygen atoms of the molecule (see Fig. 1). The following three hypotheses were made: the observed structure is (1) an artefact due to the basis set superposition error, (2) a C—H...X^--type hydrogen-bonded complex, or (3) an electrostatically stabilized pair of chemically unbound species.

The validation of the first hypothesis by the counterpoise method showed that our calculations are affected by the basis set superposition error. However, this error is not sufficiently high (3—5 kcal mol^{-1}) to explain the relatively strong interaction between the reagents. Thus, the calculated binding energies of structures **2**, **3**, **7**, and **8** are in the range of 13—15 kcal mol^{-1}.

To examine the second hypothesis, the topological analysis of the electron densities in these structures was performed by the AIM method.[16,18] The principal results given in Table 3 provide convincing evidence for the formation of a C—H...X^- hydrogen bond (X is the Cl or O atom in intermediate **5**). The AIM analysis of all the structures under consideration revealed the H...X bond path and the corresponding critical point. The electron densities ρ and the Laplacians $\nabla^2\rho$ (see Table 3) are characteristic of typical hydrogen bonds.[18] The hydrogen bond formation is evidenced also by the characteristic interatomic H...X contacts, an increase in the positive charge on the H atom, an elongation (by 0.006—0.015 Å) of the C—H bond, and a decrease in the stretching frequency of this bond.

However, the high binding energy in the complexes under study, which is absolutely untypical of weak C—H...X hydrogen bonds,[19,20] should be taken into account. Even

* Structural isomers, which differ in the mutual arrangement of the trifluoromethyl groups of the anion and dioxirane, are possible for compounds **7** and **8**. The most stable (by ~0.5 kcal mol^{-1}) structures are shown in Fig. 1.

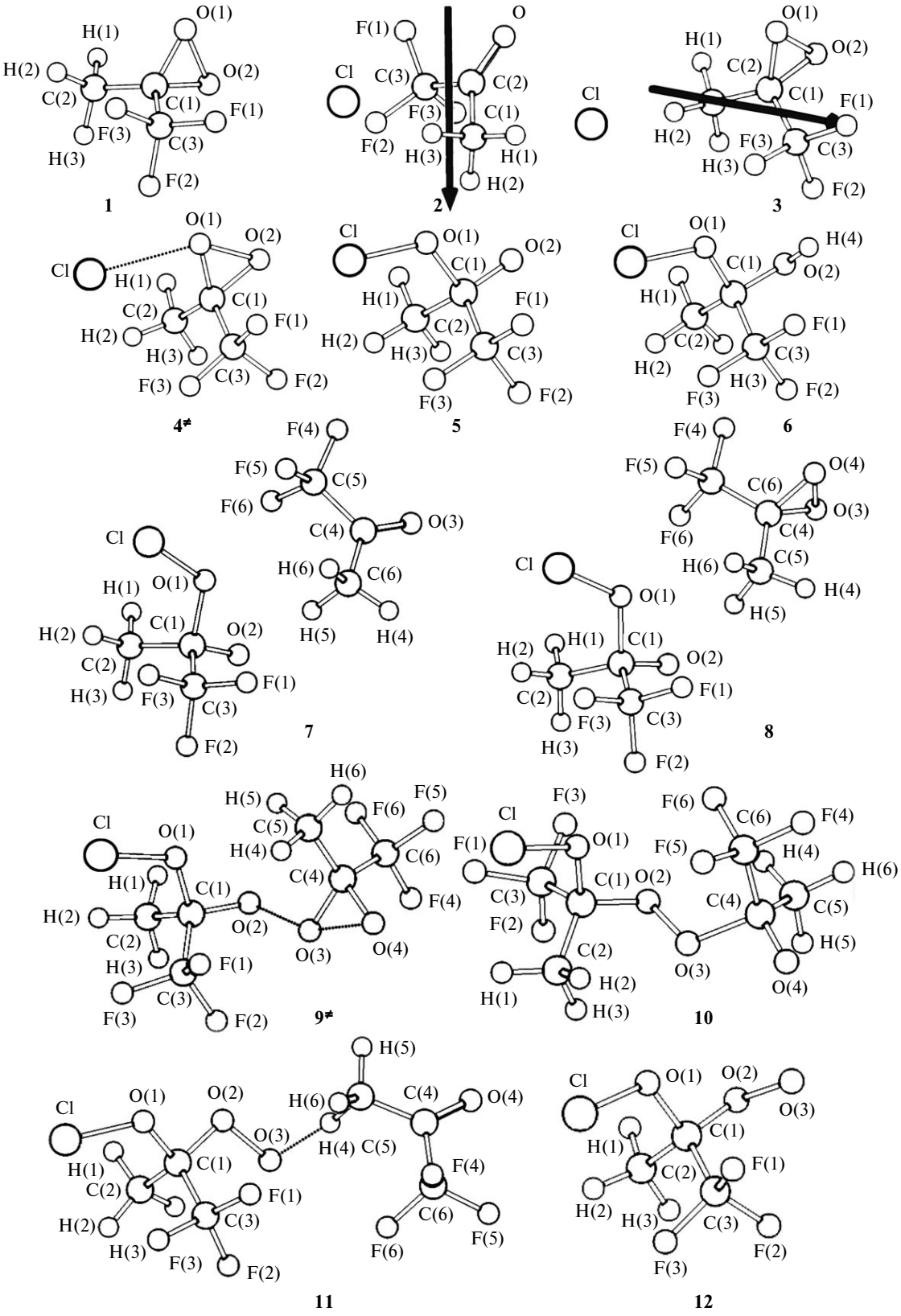

Fig. 1. Structures of dioxirane **1**, complexes **2**, **3**, **7**, and **8**, intermediates **5**, **6**, **10**, **11**, and **12**, and transition states $\mathbf{4}^{\neq}$ and $\mathbf{9}^{\neq}$ located on the singlet potential energy surface by the MP2/6-31+G(d) method for the reaction of dioxirane with chloride ions. The dipole moment vectors of complexes **2** and **3** are indicated by arrows.

Table 1. Geometric parameters of structures **1—3**, **5—8**, **10—12**, **4**$^{\neq}$, and **9**$^{\neq}$ optimized by the MP2/6-31+G(d) method

Structure	Distance	*r*/Å	Angle	φ/deg
1	C(1)—C(2)	1.496	C(2)—C(1)—C(3)	116.4
	C(1)—O(1)	1.398	O(1)—C(1)—O(2)	67.1
	O(1)—O(2)	1.547		
	C(2)—H(1)	1.091		
	C(3)—F(1)	1.338		
2	C(1)—C(2)	1.485	C(1)—C(2)—C(3)	116.1
	C(2)—O	1.227	O—C(2)—Cl	117.5
	C(2)—Cl	3.875		
3	C(1)—C(2)	1.487	C(2)—C(1)—C(3)	116.6
	O(1)—C(1)	1.400	O(1)—C(1)—Cl	97.2
	O(1)—O(2)	1.546	O(1)—C(1)—O(2)	66.8
	C(1)—Cl	4.205		
4$^{\neq}$	C(1)—O(1)	1.377	C(2)—C(1)—C(3)	115.1
	C(1)—O(2)	1.407	C(1)—O(1)—Cl	95.3
	C(1)—C(2)	1.497	O(1)—C(1)—O(2)	70.7
	O(1)—O(2)	1.610		
	O(1)—Cl	2.724		
5	C(1)—O(1)	1.599	C(2)—C(1)—C(3)	111.1
	C(1)—O(2)	1.280	C(1)—O(1)—Cl	120.9
	C(1)—C(2)	1.532	O(1)—C(1)—O(2)	103.6
	O(1)—O(2)	2.271		
	O(1)—Cl	1.746		
6	C(1)—O(1)	1.449	C(2)—C(1)—C(3)	113.0
	C(1)—O(2)	1.392	C(1)—O(1)—Cl	115.8
	C(1)—C(2)	1.508	O(1)—C(1)—O(2)	103.0
	O(1)—O(2)	2.224	H(4)—O(2)—C(1)	108.6
	O(1)—Cl	1.725		
	H(4)—O(2)	0.980		
7	Cl—O(1)	1.745	C(2)—C(1)—C(3)	111.4
	O(1)—C(1)	1.571	C(1)—O(1)—Cl	120.6
	C(1)—C(3)	1.551	O(1)—C(1)—O(2)	103.1
	C(1)—O(2)	1.291	C(5)—C(4)—C(6)	116.7
	O(1)—O(2)	2.247	C(1)—O(2)—C(4)	113.7
	O(2)—C(4)	3.911	O(2)—C(4)—O(3)	131.8
	C(4)—C(5)	1.550		
	C(4)—O(3)	1.229		
8	Cl—O(1)	1.744	C(2)—C(1)—C(3)	111.5
	O(1)—C(1)	1.582	C(1)—O(1)—Cl	120.8
	C(1)—C(3)	1.551	O(1)—C(1)—O(2)	103.2
	C(1)—O(2)	1.288	C(5)—C(4)—C(6)	117.1
	O(1)—O(2)	2.257	O(3)—C(4)—O(4)	66.6
	O(2)—O(3)	4.765	C(1)—O(2)—O(3)	126.2
	O(3)—O(4)	1.545	O(2)—O(3)—O(4)	106.2
	C(4)—O(3)	1.405		
	C(4)—C(5)	1.487		
9$^{\neq}$	Cl—O(1)	1.745	C(2)—C(1)—C(3)	110.7
	O(1)—C(1)	1.505	C(1)—O(1)—Cl	117.4
	C(1)—C(3)	1.559	O(1)—C(1)—O(2)	103.0
	C(1)—O(2)	1.324	C(5)—C(4)—C(6)	112.9
	O(1)—O(2)	2.217	O(3)—C(4)—O(4)	80.4
	O(2)—O(3)	1.972	C(1)—O(2)—O(3)	112.3
	O(3)—O(4)	1.775	O(2)—O(3)—C(4)	106.6
	O(3)—C(4)	1.365		
	C(4)—O(4)	1.385		
10	Cl—O(1)	1.728	C(2)—C(1)—C(3)	111.7
	O(1)—C(1)	1.456	C(1)—O(1)—Cl	115.7
	C(1)—C(3)	1.541	O(1)—C(1)—O(2)	103.8
	C(1)—O(2)	1.385	C(5)—C(4)—C(6)	110.8
	O(1)—O(2)	2.236	O(3)—C(4)—O(4)	103.3
	O(2)—O(3)	1.505	C(1)—O(2)—O(3)	106.4
	O(3)—O(4)	2.255	O(2)—O(3)—C(4)	115.2
	O(3)—C(4)	1.584		
	C(4)—O(4)	1.283		
11	Cl—O(1)	1.723	C(2)—C(1)—C(3)	111.4
	O(1)—C(1)	1.464	C(1)—O(1)—Cl	115.9
	C(1)—C(3)	1.555	O(1)—C(1)—O(2)	98.3
	C(1)—O(2)	1.381	C(5)—C(4)—C(6)	115.4
	O(1)—O(2)	2.153	C(1)—O(2)—O(3)	104.0
	O(2)—O(3)	1.488	O(2)—O(3)—H(4)	88.1
	O(3)—H(4)	1.843		
	C(4)—C(5)	1.477		
	C(4)—O(4)	1.230		
12	C(1)—O(1)	1.482	C(2)—C(1)—C(3)	111.4
	C(1)—O(2)	1.348	C(1)—O(1)—Cl	115.9
	C(1)—C(2)	1.522	O(1)—C(1)—O(2)	104.4
	O(1)—O(2)	2.238	O(3)—O(2)—C(1)	110.0
	O(2)—O(3)	1.480		
	O(1)—Cl	1.735		

Table 2. Torsion angles in structures **6**, **8**, **9**$^{\neq}$, and **10—12** optimized by the MP2/6-31+G(d) method

Structure	Angle	θ/deg
6	H(4)—O(2)—C(1)—O(1)	54.5
8	C(1)—O(2)—O(3)—C(4)	24.7
9$^{\neq}$	C(1)—O(2)—O(3)—C(4)	120.3
10	C(1)—O(2)—O(3)—C(4)	−140.2
11	C(1)—O(2)—O(3)—H(4)	−128.4
	O(3)—O(2)—C(1)—O(1)	167.1
12	O(3)—O(2)—C(1)—O(1)	76.4

in cyclic dimers of carboxylic acids, the hydrogen bond energy for strong O—H...O hydrogen bonds is ~7 kcal mol^{-1} (see Ref. 21), which is substantially lower than the binding energies in complexes **2**, **3**, **7**, and **8** (see Table 3).

Hence, we suggested that the complexes under consideration are stabilized not only by weak hydrogen bonding but also by electrostatic factors, in particular, by ion-dipole interactions. Actually, in all the structures the orientation of the vector of the dipole moment of the polar molecule with respect to the ion (for example, see Fig. 1, structures **2** and **3**) is favorable for the ion-dipole interaction, which is consistent with the electrostatic nature of the binding.

Table 3. Energies of ion-dipole interactions E_{i-d}, the enthalpies of complex formation $\Delta_r H^o$, the equilibrium C—H...X hydrogen bond lengths, the electron densities ρ, and the Laplacians of the electron densities $\nabla^2\rho$ at the critical points of the H...X bond path

Complex	$-E_{i-d}$	$-\Delta_r H^o$ [a]	r(C—H)	r(H...X)	ρ [b]	$\nabla^2\rho$ [b]
	kcal mol^{-1}		Å		a.u.	
2	9.9	10.7	1.110	2.307	0.022	0.066
3	9.9	10.2	1.104	2.343	0.020	0.062
7	9.4	10.1	1.107	2.019	0.024	0.077
8	4.7	9.9	1.100	2.095	0.021	0.068

[a] The thermal effect of the reaction with the correction for the basis set superposition error is 2.9—4.9 kcal mol^{-1} depending on the nature of the complex.
[b] The ranges of the values characterizing the formation of typical hydrogen bonds are 0.002—0.035 for the electron density and 0.024—0.139 for the Laplacian.[18]

The energies of the ion-dipole interactions (E_{i-d}) in the structures under consideration were evaluated according to the equation

$$E_{i-d} = -\frac{1}{4\pi\varepsilon\varepsilon_0}\cdot\frac{q\mu\cos\theta}{r^2},$$

where ε is the dielectric constant of the medium (ε = 1), ε_0 is the vacuum dielectric constant, q is the charge of the ion, μ is the dipole moment of the molecule under consideration, r is the distance between the ion and the center of the dipole, and θ is the angle between the vector $\boldsymbol{r}$ and the axis of the dipole. The coordinates of the center of the dipole were calculated in the point charge approximation for polar molecules. The point charges were found based on the analysis of the electron density distribution by the NBO method.

As can be seen from Table 3, the energies of ion-dipole interactions calculated in the point charge approximation are similar to the enthalpies of formation of complexes **2**, **3**, **7**, and **8** ($\Delta_r H^o$) evaluated by quantum chemical methods and corrected by the counterpoise method. Therefore, the analysis of the nature of binding of the species in these complexes shows that the ion-dipole interactions play the main role, whereas the C—H...X hydrogen bond makes a minor contribution.

Mechanism of singlet oxygen generation. The located set of stationary points on the potential energy surface for the reaction under consideration suggests the following scheme of transformations, which explains the experimental observations of the catalytic decomposition of TFD accompanied by the efficient generation of singlet oxygen.[9] In a solution in TFA, the catalyst exists mainly as complex **2**.

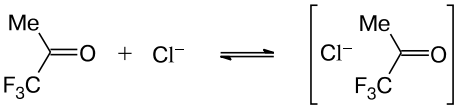

(1)

2

Hereinafter, the ion-dipole pairs are enclosed in square brackets. It should be noted that this interaction reflects the effect of the solvent on the reaction pathway of TFD with Cl^-. The enthalpy of formation of complex **2** is given in Table 3. Then the resolvation of the chloride ion by dioxirane occurs (reaction (2)).

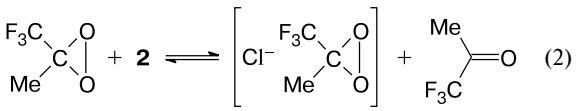

(2)

This reaction is almost thermally neutral (Table 4). Hence, due to a considerable difference in the concentrations of the molecular components, the equilibrium of reaction (2) is shifted to the left. However, due to the low activation energy, complex **3** is rapidly transformed into intermediate **5** through the dioxirane ring opening, resulting in the irreversible consumption of dioxirane.

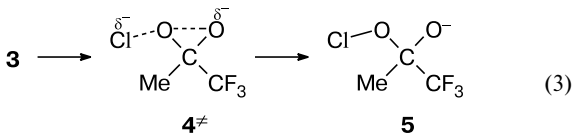

(3)

4≠ **5**

Reaction (3) is the first step in the catalytic decomposition of TFD. In intermediate **5**, the C—O^- bond length is 1.280 Å, which is substantially smaller than the corresponding bond length in compound **1** (1.398 Å).

There are two possible transformation pathways of intermediate **5**. One pathway involves the decomposition of intermediate **5** into TFA and the hypochlorite ion, which is a chain carrier in the catalytic decomposition of dioxiranes according to the mechanism proposed in the study:[9]

Table 4. Enthalpies and Gibbs free energies for the steps of the formation of singlet oxygen during the chloride ion-induced decomposition of dioxirane **1**

Step	$\Delta_r H°_{298.15\,K}$	$\Delta_r G°_{298.15\,K}$
	kcal mol^{-1}	
1	−10.7	−4.6
2	0.5	0.1
3	−17.6	−15.4
	−1.2[a]	1.0[a]
4	34.6	22.1
5	−10.1	−0.4
6	0.2	−0.1
7	−4.0	0.8
	2.8[a]	5.7[a]
8	16.3[a]	12.7[a]
9	17.7[a]	7.9[a]
10	−51.5[b]	−67.2[b]

[a] Calculated at the MP2/6-31+G(d) level of theory.
[b] Calculated with respect to the ground state of the O_2 molecule ($^3\Sigma_g^-$).

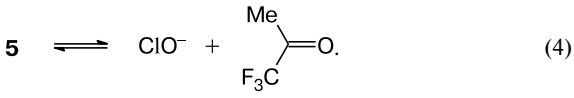

(4)

Another pathway involves the formation of ion-dipole pair **7** (reaction (5)) followed by the resolvation of the complex anion by the TFD molecule to form complex **8** (reaction (6)).

(5)

7

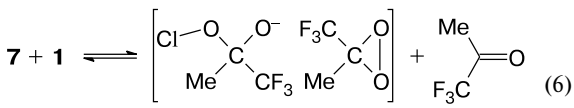

(6)

8

The monomolecular decomposition of intermediate **5** is 34.6 kcal mol^{-1} endothermic (see Table 3), ΔG° = = 22.1 kcal mol^{-1}. Taking into account $\Delta G^\circ = -RT\ln K_p$ and $K_c = K_p(RT)^{-\Delta\nu}$, we calculated the equilibrium constant K_c and estimated the ratio of the concentrations of the anionic forms involved in reaction (4) as [**5**]/[ClO$^-$] = = [TFA]/$K_c = 5 \cdot 10^{18}$. Therefore, the decomposition of intermediate **5** in TFA is thermodynamically unfavorable. Hence, the chain of the transformations (5) and (6) seems to be virtually the only transformation channel of intermediate **5**.

Reactions (5) and (6) are similar to reactions (1) and (2). Their thermal effects are given in Tables 3 and 4. As in the case of complex **3**, the relief of the strain in the dioxirane ring is the driving force of the transformation of ion-dipole pair **8**, due to which reaction (7) is strongly exothermic (see Table 4).

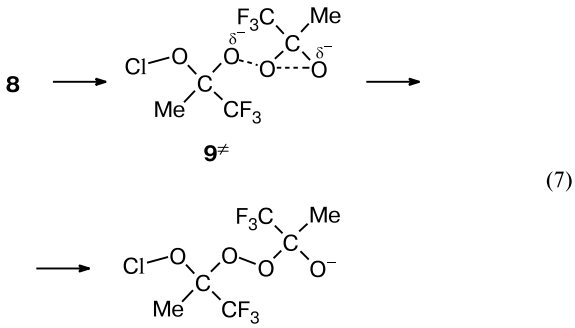

(7)

9$^{\neq}$

10

Reaction (7) is the second step of the catalytic decomposition of dioxirane giving unstable energy-saturated intermediate **10** overcrowded with electronegative atoms. The successive decomposition of intermediate **10** is an important process of the generation of singlet-excited oxygen. Initially, the elimination of TFA occurs to form key structure **12**, which is the direct precursor of singlet oxygen:

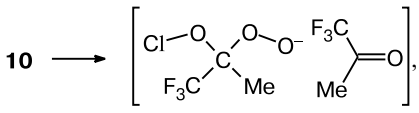

(8)

11

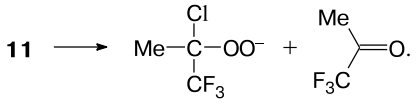

(9)

12

We did not locate the transition state of this transformation. However, taking into account the smooth potential energy surface of this reaction estimated by the scan with the use of the MP4//MP2 method, the decomposition of intermediate **10** should be very fast. Then peroxide intermediate **12** releases the singlet oxygen molecule and regenerates the catalyst for the reaction, *viz.*, the chloride ion solvated by a TFA molecule:

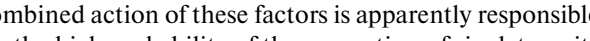

(10)

Based on the theoretical modeling of the chloride ion-induced decomposition of compound **1**, we proposed the stepwise mechanism of the process described by reactions (1)—(10). Earlier,[8,9] the similar mechanism has been described for the catalytic decomposition of DMD. Therefore, the replacement of the methyl group in dioxirane by CF_3 has only a qualitative effect on the process, which is reflected in a slight change in the thermal effects of individual steps.

The mechanism proposed in the present study is characterized by the following features: (a) the formation of relatively stable complexes of the catalyst or its oxidized form with the dioxirane molecule (or a solvent), which apparently facilitate the mutual orientation of the reagents in the catalytic transformation, (b) the low activation barriers and highly exothermic key steps of the process, and (c) the fact that all transformations up to the generation of $^1O_2$ occur on the singlet potential energy surface. The combined action of these factors is apparently responsible for the high probability of the generation of singlet-excited molecular oxygen[5,22—30] in the reaction under consideration.

It is interesting to compare the mechanism proposed in the present study with the earlier mechanistic description of the pathways of this process[8,9] shown in Scheme 1. The important difference between the two mechanisms is the nature of the oxidized form of the catalyst and, as a consequence, the structure of the precursor of singlet oxygen (intermediate **A** in Scheme 1). Our results provide unambiguous evidence for the extremely low thermodynamic probability of the existence of free hypochlorite ions in TFA.

The fact that we failed to locate the structure **A** as a stable chemical compound or the possible transition state

of the reaction is an additional argument in favor of the new mechanism of the chloride ion-induced decomposition of compound **1**. In addition, unlike the mechanism shown in Scheme 1, the sequence of transformations (1)—(10) includes the association of the reagents and intermediates with the solvent, which provides at least the partial account for the effect of the medium.

In the study,[31] it was concluded that a decrease in the yield of singlet oxygen in the reaction under consideration can be attributed to the one-electron transfer from the catalyst to dioxirane:

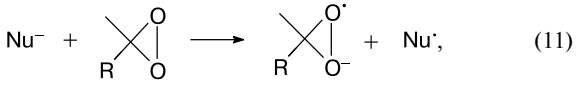

where Nu is a nucleophilic agent and R is Me or CF_3. In the course of this reaction, the catalyst is irreversibly consumed, and the decomposition of dioxirane can occur bypassing the path, in which singlet oxygen is generated.

To explain the factors responsible for the high yield of O_2 ($^1\Delta_g$) in the reaction under consideration, we calculated the electron affinities (EA) for dioxiranes and a series of reduced catalytic forms of Nu by the G3MP2B3 method (Table 5). This method reproduced the experimental values of EA with high accuracy, which is indicative of the reliable estimate of these values for dioxiranes and intermediate **5**.

The high efficiency of the generation of $^1O_2$ for DMD and compound **1** is attributed to the ability of the Cl^- ion and intermediate **5** to hold an extra electron, which decreases the probability of side reaction (11). The results presented in Table 5 additionally confirm the validity of the mechanism of the catalytic decomposition of dioxiranes resulting in the efficient generation of singlet oxygen proposed earlier[13] and in the present study. If the reaction proceeded with the involvement of the hypochlorite ion, the one-electron transfer (11) would be efficient for at least dioxirane **1**, which is inconsistent with the experimental data.

Table 5. Electron affinities of dioxiranes and reduced forms of potential catalysts for the decomposition of dioxiranes

Compound	EA/eV	
	Calculation[a]	Experiment[b]
	1.87	—
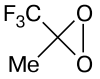	2.74	—
Cl	3.69	3.614
ClO	2.32	2.278
Cl_2	2.45	2.42±0.10[c]
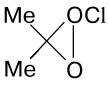	2.77	—
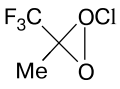	3.60	—

[a] Calculations by the G3MP2B3 method.
[b] NIST Chemistry WebBook; http://webbook.nist.gov.
[c] The average value for eight measurements.

The experimentally observed quenching of $^1O_2$ with acid[9] can be explained in terms of this mechanism. Actually, the protonation of intermediate **5** giving compound **6** (see Fig. 1) in fact means the catalyst poisoning. The protonation of dioxirane, which is finally also reflected in the mechanism of the reactions of compounds **5** and **1** (reactions (1)—(10)), is another possible factor responsible for the action of acids inhibiting the generation of $^1O_2$. Finally, the acidic medium facilitates redox transformations. Consequently, there is a higher probability of side reactions (11), resulting in a decrease in the yield of singlet oxygen in the reaction under consideration.

Based on the above-described model of the process, suggestions can be made about the influence of different factors on the efficiency of the generation of $^1O_2$ and about the characteristic features of the reaction. First, the kinetic analysis of the sequence of reactions (1)—(10) assuming the quasi-stationary concentration of intermediate **5** shows that this process is characterized by the first order with respect to the concentrations of Cl^- ions and dioxirane. Second, taking into account the direct involvement of the solvent (TFA) in this process, the medium has apparently a considerable effect on the yield of $^1O_2$. This effect can be manifested both in the change in the concentration of ketone (which is always present in the system due to the decomposition of dioxirane) and the control of the activity of the catalyst due to specific interactions with the solvent. Third, the mechanism assumes the considerable influence of the anion.

Actually, there is a general tendency for a decrease in the yield of $^1O_2$ in the series of anions used for the decomposition of dioxiranes (Cl^-—Br^-—I^-—Me_3CO^-—HO^-),[8,9] which is attributed to the fact that the probability of the redox pathway of this reaction increases in this series.[31] According to our data, the effective catalyst providing a high yield of singlet oxygen should have high ionization potentials (which is equivalent to the high EA of the reduced state) for both catalytic forms. The chloride ion and its oxidized catalytic form **5** meet these requirements, which is confirmed by the exceptionally efficient, nearly quantitative, generation of singlet oxygen during the chloride ion-induced decomposition of dioxiranes.

To sum up, high-energy peroxides, *viz.*, dioxiranes,[2,10,11,32,33] efficiently generate singlet oxygen during their chloride ion-induced decomposition. In this unique

catalytic process, one of the most efficient chemiluminescent transformations of dioxiranes occurs.[5] According to quantum chemical calculations, this catalytic process is complex and the hypochlorite ion proposed earlier[9] is not a chain carrier in the reaction. Intermediate **12** rather than the intermediate **A**, which has been postulated earlier (Scheme 1), is the direct precursor of the oxygen molecule in the excited electronic state.

This study was financially supported in part by the Russian Foundation for Basic Research (Project No. 09-03-00831-a), the Council on Grants at the President of the Russian Federation (Program for State Support of Young Doctors, Grant MD-3852.2009.3), and the Division of Chemistry and Materials Science of the Russian Academy of Sciences (Program No. 1-OKh).

References

1. W. Murray, *Chem. Rev.*, 1989, **89**, 1187.
2. V. P. Kazakov, A. I. Voloshin, D. V. Kazakov, *Usp. Khim.*, 1999, **68**, 283 [*Russ. Chem. Rev.* (*Engl. Transl.*), 1999, **68**, 253].
3. W. Adam, C. R. Saha-Müller, C.-G. Zhao, *Org. React.*, 2002, **61**, 219.
4. W. Adam, K. Brivida, F. Duschek, D. Golsch, W. Kiefer, H. Sies, *J. Chem. Soc., Chem. Commun.*, 1995, **18**, 1831.
5. W. Adam, D. V. Kazakov, V. P. Kazakov, *Chem. Rev.*, 2005, **105**, 3371.
6. M. Ferrer, F. Sanchez-Baeza, A. Messeguer, W. Adam, D. Golsch, W. Kiefer, V. Nagel, *Eur. J. Org. Chem.*, 1998, **11**, 2527.
7. V. Nagel, F. Duschek, W. Kiefer, F. Görth, D. Golsch, W. Adam, M. Ferrer, A. Messeguer, *Asian J. Spectrosc.*, 1998, **2**, 35.
8. W. Adam, W. Kiefer, S. Schlücker, C. Saha-Müller, D. V. Kazakov, V. P. Kazakov, R. R. Latypova, *Bioluminescence and Chemiluminescence: Progress and Current Applications*, Ed. P. E. Stanley, L. J. Krucka, World Scientific Publishing, Singapore, 2002, 129.
9. W. Adam, D. V. Kazakov, V. P. Kazakov, W. Kiefer, R. R. Latypova, S. Schlücker, *Photochem. Photobiol. Sci.*, 2004, **3**, 182.
10. D. V. Kazakov, V. P. Kazakov, G. Y. Maistrenko, D. V. Mal´zev, R. Schmidt, *J. Phys. Chem. A*, 2007, **111**, 4267.
11. D. V. Kazakov, A. B. Barzilova, V. P. Kazakov, *Chem. Commun.*, 2001, 191.
12. D. V. Kazakov, A. I. Voloshin, N. N. Kabal´nova, V. V. Shereshovets, V. P. Kazakov, *Mendeleev Commun.*, 1998, **2**, 49.
13. M. Yu. Ovchinnikov, S. L. Khursan, D. V. Kazakov, W. Adam, *J. Photochem. Photobiol. A: Chem.*, 2010, **210**, 100.
14. L. A. Curtiss, P. C. Redfern, K. Raghavachari, V. Rassolov, J. A. Pople, *J. Chem. Phys.*, 1999, **110**, 4703.
15. J. P. Foster, F. Weinhold, *J. Am. Chem. Soc.*, 1980, **102**, 7211.
16. R. F. W. Bader, *Atoms in Molecules: A Quantum Theory*, Clarendon Press, Oxford, 1990.
17. M. J. Frisch, G. W. Trucks, H. B. Schlegel, G. E. Scuseria, M. A. Robb, J. R. Cheeseman, V. G. Zakrzewski, J. A. Jr. Montgomery, R. E. Stratmann, J. C. Burant, S. Dapprich, J. M. Millam, A. D. Daniels, K. N. Kudin, M. C. Strain, O. Farkas, J. Tomasi, V. Barone, M. Cossi, R. Cammi, B. Mennucci, C. Pomelli, C. Adamo, S. Clifford, J. Ochterski, G. A. Petersson, P. Y. Ayala, Q. Cui, K. Morokuma, D. K. Malick, A. D. Rabuck, K. Raghavachari, J. B. Foresman, J. Cioslowski, J. V. Ortiz, A. G. Baboul, B. B. Stefanov, G. Liu, A. Liashenko, P. Piskorz, I. Komaromi, R. Gomperts, R. L. Martin, D. J. Fox, T. Keith, M. A. Al-Laham, C. Y. Peng, A. Nanayakkara, M. Challacombe, P. M. W. Gill, B. Johnson, W. Chen, M. W. Wong, J. L. Andres, C. Gonzalez, M. Head-Gordon, E. S. Replogle, J. A. Pople, *Gaussian 03 Revision-D02*, Gaussian Inc., Pittsburgh PA, 2004.
18. I. S. Bushmarinov, K. A. Lysenko, M. Yu. Antipin, *Usp. Khim.*, 2009, **78**, 307 [*Russ. Chem. Rev.* (*Engl. Transl.*), 2009, **78**].
19. U. Koch, P. L. A. Popelier, *J. Phys. Chem. A*, 1995, **99**, 9747.
20. S. Scheiner, S. J. Grabowski, T. Kar, *J. Phys. Chem. A*, 2001, **105**, 10607.
21. G. C. Pimentel, A. L. McClellan, *The Hydrogen Bond*, W. H. Freeman and Co, San Francisco—London, 1960.
22. H. H. Wasserman, R. W. Murray, *Organic Chemistry: Singlet Oxygen*, Academic Press, New York, 1979, **40**.
23. A. A. Frimer, *Singlet Oxygen*, CRC: Boca Raton, Florida, 1985.
24. W. Adam, T. Wirth, *Acc. Chem. Res.*, 1999, **32**, 703.
25. C. Schweitzer, R. Schmidt, *Chem. Rev.*, 2003 **103**, 1685.
26. J. Cadet, J.-L. Ravanat, G. R. Martinez, M. H. G. Medeiros, P. Di Mascio, *Photochem. Photobiol.,* 2006, **82**, 1219.
27. E. Skovsen, J. W. Snyder, P. R. Ogilby, *Photochem. Photobiol.*, 2006, **82**, 1187.
28. R. Schmidt, *Photochem. Photobiol.*, 2006, **82**, 1161.
29. A. A. Krasnovskii Jr., *Biokhimiya*, 2007, **72**, 1311 [*Biochemistry (Moscow)* (*Engl. Transl.*), 2007, **72**, 1065].
30. B. F. Minaev, *Usp. Khim.*, 2007, **76**, 1059 [*Russ. Chem. Rev.* (*Engl. Transl.*), 2007, **76**, 989].
31. M. Yu. Ovchinnikov, S. L. Khursan, D. V. Kazakov, V. P. Kazakov, *Vestn. Bashkirsk. Un-ta.* [*Vestn. Bashk. Univ.*], 2008, **13**, 789 (in Russian).
32. W. Adam, R. Curci, J. O. Edwards, *Acc. Chem. Res.*, 1989, **22**, 205.
33. W. Adam, R. Curci, *Chim. Ind. (Milan)*, 1981, **63**, 20.

Received May 14, 2010